Development of a Pattern Making Method for Strain Measurement on Microstructural Level in Ferritic Cast Iron

Keivan A. Kasvayee[1,a], Lennart Elmquist[1,2], Anders E.W. Jarfors[1] and Ehsan Ghassemali[1]

[1]School of Engineering, Jönköping University, Box 1026, 551 11 Jönköping, Sweden
[2]Sinter Cast AB, Technical Centre, Kungsgatan 2, 641 30 Katrineholm, Sweden

Abstract

The current paper focuses on development of a method for studying micro-scale strains on the microstructure of ferritic cast iron. For this purpose, in-situ tensile tests were done under the optical microscope combined with digital image correlation (DIC). Critical in this development was to be able to achieve a reliable high spatial resolution of strain around microstructural features, such as graphite particles. Measurement of local strain fields in cast iron materials have so far been relying on displacement of naturally occurring microstructure patterns such as graphite particles, which limits the spatial resolution of strain measurement. In order to increase the spatial resolution of the measured strain, a pit etching procedure was applied to generate a random speckle pattern on the ferritic matrix. The critical challenges of in-situ investigation of microstructural deformation were identified as speckle pattern quality and accurate selection of subset size and strain window size. The traceability of this method was studied by benchmarking the measured elastic modulus with that obtained from full-scale tensile test. The elastic modulus calculated from average strains, measured by DIC, showed a good agreement with material's elastic modulus. This validates the measured localized strain values and can be used as a validation for modeling of local deformation.

Keywords: Ferritic cast iron, Digital image correlation (DIC), In-situ tensile test, Pit etching, Subset size, Strain window size

1 INTRODUCTION

The combination of digital image correlation (DIC) and optical microscopy is a relatively new method for determining full-field displacement and strain at micro-scale level [1, 2]. DIC is an optical-numerical pattern tracking technique which requires a random, firmly-bonded, high contrast and appropriately sized speckle pattern on the surface of an object to compute displacement and strain by comparing a series of digitized images [1, 3, 4]. However, generating a suitable speckle pattern in microscopic level without harming the microstructure of material is still challenging. Speckles mustbe small enough to enable measurements in between and around microstructural features. So far, pattern generation methods in the micro-scale level has

[a]Corresponding author: **Email:** Keivan.Amiri-Kasvayee@jth.hj.se

been based on photolithography [5], chemical vapor thin film patterning [5], laser patterning [6] micro/nano particles [2, 7, 8], fine paint [8, 9], etching and using natural microstructural pattern [10, 11]. However, many of these common techniques for patterning in reduced length scale suffer from high costs, relatively long procedure, need for special equipment, need of elaboration, destruction of the original microstructure, inadequatespatial resolution, inaccuracy and low repeatability [5, 7].

In cast iron materials,natural microstructural pattern and fine painting have been used as speckle pattern making techniques for DIC [9, 12]. Natural microstructural patterns are a combination of patterns that are obtained by etching (such as pearlite, ferrite and grain boundaries) and microstructure features (such as graphite, inclusion and micro porosities). Using natural microstructural pattern for cast iron materials can induce uncertainty in DIC computations. In this regard, the linear shape of grain boundaries and pearlite layers raise the correlation errors along the line, where the detection ofthe gradient becomes impossible [13]. Moreover, gradient detection inside ferrite and graphite areas is almost impossible due to the absent of speckle patterns. This effect is even more problematic in fully ferritic cast irons where the matrix appears fully white in microscope pictures. In this case, the only choice is to use graphite particles as speckle patterns. However, this will limit the local gradient detection within and around graphite particles [14], where the critical regions for crack nucleation and growth locate [15]. Further more, using fine paint as a speckle pattern, masks the beneath microstructure features. For example, it would be very difficult to distinguish DIC results relating to grain boundaries regions due to the masking effect of paint particles [9].

As an alternative, pit etching technique is introduced in this paper as a new method for generating microscale speckle pattern on the surface of ferritic cast iron. Pit etching has been normally used as a technique for determining grain size distribution, grains orientation and dislocation density on the surface of polycrystalline materials [16, 17]. In this technique, an etchant produces pits on the surface of material where the local defects such as dislocations, vacancies, inclusions, or impurities exist. Depending on the crystallographic orientation of the grains, the pits demonstrate different geometries and appear as dark spots on the microstructure. Accordingly, in this study pit etching was adapted for digital image correlation, and pits were considered as the speckle pattern for local strain measurement within the grains and around graphite particles.

The aim of this paper was to verify the feasibility of applying pit etching as a pattern generating method to increase spatial resolution for measuring micro-scale deformation using DIC technique. For this purpose, a pit etching procedure was developed and applied on cast iron samples to produce microscale speckle pattern. Optical microscope pictures were taken at two different magnifications. Two different speckle patterns were used: (i) pits and (ii) natural microstructural pattern. Aminimum DIC subset size was defined depending on the speckles' size and distribution. Displacement and strain spatial resolution together withstand ard deviation were computed for therecorded images using a DIC software. In-situ tensile tests under optical microscope were per formed and series of real-time deformation images were recorded to verify the results. The deformation images were investigated by DIC and their average strains were used for calculation of the material's elastic modulus.

2 EXPERIMENTAL PROCEDURE

2.1 Material

Ahigh silicon cast iron with the chemical composition given in Table 1 was used in this study. Samples were cut from a 30 mm thick cast plate (240 × 140 × 30 mm). The microstructure of the material consisted of nodular and vermicular graphite embedded in a fully ferritic matrix (Fig. 1). The high amount of silicon (3.7 wt.%) stabilized the ferrite phase in the cast material [18]. Nodularity (by area) was measured as 67.4% based on the ASTM E 2567 [19].

Table 1 Chemical composition of the cast material

Element	C	Si	Mg	Mn	P	S	Sb	Ce	Fe
Weight percent (Wt.%)	3.28	3.73	0.037	0.169	0.009	0.004	0.006	0.002	Balanced

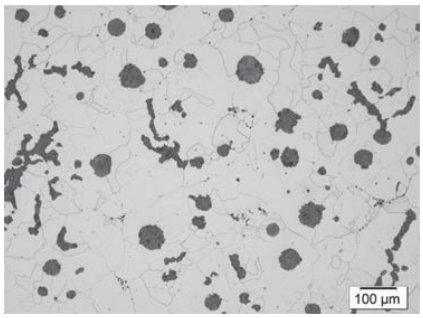

Fig. 1 Optical micrograph of the cast material, etched with 5% nital.

2.2 Testing Equipment

An invert optical microscope (Olympus GX81) equipped with aCCDcamera (Olympus UC30) was used for recording the patterned surfaces and deformation images. Images were recorded in gray scale with the size of 2080 × 1544 pixels giving 15.4 and 0.96 mm^2 field of view (2.19 and 0.54 µm/pixel) for 15.8X and 63X nominal magnification, respectively.

The tensile tests were performed using a miniature tensile stage produced by TSL Solutions KK, Japan. The machine is designed for double direction uniaxial tensile load with the maximum load cell capacity of 1200 N. Figure 2(a) shows the micro tensile specimen adopted for the tensile test machine. The tensile samples were machined from the cast plate and were grinded to 1 mm in thicknessto enable the tensile testing in the range of maximum load capacity. In order to obtain accurate strain results, a machine stiffness correction was made after assessing the tensile stage spring constant [20].

The miniature tensile stage was installed in the optical microscope for in-situ tensile testing (Figure 2(b)). Specimens were grinded and polished before the tensile test. In total, 20 specimens were produced of which 10 were pit etched (reagent A in Table 2). For each combination of etching situation (etched or un-etched) and magnification (15.8X or 63X) five samples were tested. The image window was placed approximately at the middle section of the specimens'

gage length to minimize the movement of initial area to outside of the field of view. The tensile test was done at a grip displacement rate of 3.3 μm/s up tofracture. Overall stress-strain behavior of samples was measured based on the axial force and the grip displacement and data were recorded every second. Simultaneously, deformation images were captured by the microscope every 4 seconds using autofocusing after each record. Autofocusing process enabled real time image recording without pausing the tension process. The stress at the time of image recording could be defined by coupling the recorded times.

Table 2 Pit etch reagents compositions

Reagent	*Chemical composition (Vol.%)*
A	0.2%HCl + 2%H_2O_2 + 97.8% H_2O
B	5%HF + 95%H_2O_2

In order to benchmark elastic modulus results obtained from DIC and in-situ tensile testing, five tensile samples were machined from the cast plate and tested according to ASTM E 8M [21] using Zwik/roell Z100 testing machine. In addition, the effect of pit etching on tensile properties was investigated by pit etching and tension testing of three additional standard samples. It is important noting that the results showed that pit etching had no detrimental influence on the tensile properties.

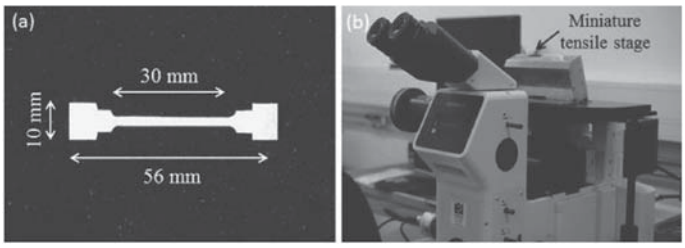

Fig. 2 (a) Specimen geometry adopted for miniature tensile stage with 1 mm thickness; (b) View of miniature tensile stage installed in the microscope for in-situ tensile testing.

2.4 Pattern Making

In order to produce pits, two pit etching reagents (A and B in Table 2) that were previously used for pure iron [22] and silicon steels [17, 23], were examined and reagent A was selected for speckle generating. Then, fifty samples with surface dimensions of 20 × 10 mm were cut from the cast plate. Samples were mounted and their surfaces were grinded and polished. Ten samples were kept as reference samples for considering graphite particles as natural microstructure pattern and the rest were pit etched according to pit etching procedure presented in Table 3. To study the effect of temperature on the number of pits, the pit etching was performed in room temperature, 50, 75 and 100°C (Table 3). The maximum temperature of heating was selected as 100°C due to the boiling temperature of water that contains a large portion of the pit etch regent. After heating, the surface of the samples was immersed in the reagent for 10 seconds for pit formation. Afine post polishing step was performed on the samples after pit etching in

order to remove the oxidations and increase the contrast in the microscopic images. Finally, ten seconds immersion in 5% Nital can be performed as an optional step to reveal the ferrite grain boundaries. However, in this study etching with Nital was not performed since the scope was to only consider pits or graphite as speckle pattern.

Depending on the etching situation, speckle patterns were categorized into five groups: (i) un-etched; pit etched at (ii) room temperature, (iii) 50°C, (iv) 75°C and (v) 100°C. Graphite particles were considered the speckle pattern in the un-etched group and in the rest of the groups pits had the speckles'role. It is important noting that when pits were considered the speckle pattern, the graphite particles were excluded from the calculation. Thespeckles'mean radius, area, nearest neighbor distance (NND) and density were measured for each group using Olympus stream motion software. The mean radius of speckles was calculated as half of the average of the shortest and longest crossing lines that passes through the center of gravity of speckle. Nearest neighbor distance was defined as the shortest distance from the center of gravity of a speckle to another speckle's gravity center. Density was the number of speckles per square millimeter of surface area. The obtained results were used to define the minimum subset size for each speckle pattern group.

Table 3 Pit etching procedure

Step 1. Mechanical polishing of sample surface
Step 2. Increasing the potential number of pits by heating samples to 50, 75 and 100°C in furnace
Step 3. Pit etching (speckle generating) by 10 seconds immersion in reagent A (Table 2)
Step 4. Removing oxidation products from the surface by fine post polishing (polishing with 15 N force with 1 μm diamond for 1 minute)
Step 5. Revealing grain boundaries by 10 seconds immersion in 5% Nital (optional)

2.3 Digital Image Correlation

In general, two types of images were analyzed by DIC in this study. First, the stationary images that were recorded from mounted samples, in which no deformation was applied. These images were used for determination of noise, spatial resolution and standard deviation of displacement and strain. Second, the deformation images that were recorded during in-situ tensile testing. In these images, the mean value of strain was measured for the entire field of view to experimentally verify the accuracy and traceability of speckle pattern.

The commercial Match ID 2D software was used for DIC analysis [24]. The program follows the subset-based method, where correlation occurs by considering a pixel and its neighborhood, specified as subset, in the undeformed image and matching the same subset in the deformed image [3, 4, 24]. Subset size determines the minimum displacement area which can be resolved. In order to achieve reliable and accurate results, subset size must be large enough to contain unique and identifiable features. Too small subset will result in high uncertainty in correlation results whereas too large subsets will smooth out details in large heterogenous deformations and significantly degrade the accuracy of the results [25, 26]. Lower limit of subset size is governed by granularity of the speckle pattern. The upper limit of subset size can be defined

depending on the desired spatial resolution. Subsets have square shapes with side length of (2N+1) pixels [24, 25].

In this study, the lower limit was defined in a manner that every subset covers at least three speckles in the entire field of view [27]. The speckles were considered randomly distributed and the side length of subset was determined according to the two-dimensional random walk. Two dimensional random walk associates to the path taken by a point or quantity that moves in a step on a plane, where the direction of each step is determined randomly [28]. Equation 1 represents the most probable distance from the initiation point after P steps in two-dimensional random walk.

$$d = r\sqrt{P} \tag{1}$$

where d is the root-mean-squared distance, r is the size of one step and P is the number of steps to distance.

Considering Eq. 1 for calculating the length of subset, NND was considered the size of step (r), and the number of steps (P) was considered 2 so that every subset contains at least 3 speckles. Consequently, root-mean-squared distance (d) would be defined as the most probable position of two random speckles around a randomly selected speckle.In addition, speckles had a notable size that mustbe consideredfor subset length calculation. Therefore, two mean values of speckles' radius were added to the root-mean-squared distance (d) for calculating the side length of subset. Eventually, the side length of subset size was calculated by using Eq. 2 for each group of speckle pattern.

$$L = ((NND + 1.95 \times SD_{NND}) - \sqrt{2}) + ((R + 1.95 \times SD_R) \times 2) \tag{2}$$

where L is the side length of the minimum subset size that can be used for the pattern, R is the mean radius of speckle patterns, SD_{NND} and SD_R are the standard deviation of nearest neighbor distance and mean radius, respectively.

The dimension of the length side obtained from Eq. 2 is in metric system and is needed to be converted to pixel for use in DIC program. This conversion was done according to pixel size in each magnification.

Noise was evaluated by DIC program for 51 stationary images recorded from the speckle patterns in both magnifications. Here, noise is the smallest measured value associated with a change of signal, which is typically related to sensitivity of the CCD camera and digitization. Noise evaluation results showed an average noise level of 0.440.1 percent for both magnifications.

Spatial resolution and standard deviation of displacement and strain were assessed for each sample in each group of speckle pattern using self-correlation method [29]. Standard deviation is the smallest value of the measured (displacement or strain) that can be detected above noise [27]. Spatial resolution is defined as the smallest distance between two independent measurement points. Displacement spatial resolution is the subset size since it defines the distance between two independent data points in correlation. The strain spatial resolution is limited by the subset size used for correlation matching and by the measurement grid of strain concentration, which can be calculated from the Eq. 3. In this equation, step size is the distance between two adjacent displacement data pointsthat were measured by DIC, which determines the data density of a displacement field. The strain window is the number of displacement data points that are involved for strain calculation. Strain window size in pixel dimension, denoted as virtual

strange gage (VSG), can be measured from Eq. 4, which represents the smoothing area for strain measurements [26, 30]. In this study, spatial resolution and standard deviation were evaluated by correlating the reference image with one stationary image in the DIC program employing the pattern's minimum subset sizes. For strain spatial resolution and standard deviation, constant step size and strain window of 5 pixels and 55 data points (VSG = 2121 pixels), respectively, were used for all the samples. The outcome was used for selection of the best speckle pattern in each magnification for in-situ tensile testing.

$$SRR = SS + [SW - 1) \times ST \quad (3)$$

$$VSG = (ST \times (SW - 1)) + 1 \quad (4)$$

where SRS is the spatial resolution of strain, SS is the step size, SW is the strain window and ST is the step size.

The effect of autofocusing was investigated by refocusing and recording images from the surface of a stationary patterned sample. The correlation was done by DIC for the refocused images. The results showed that the variation in displacement and strain upon refocusing was indistinguishable from the base line standard deviation for each pattern type. This implies that the same level of focus was maintained throughout the entire in-situ tensile testing.

Deformation images acquired from in-situ tensile testing were analyzed by DIC to compute the average strains across the field of view throughout the elastic deformation. The minimum subset sizes were used for the analysis based on the specimens' speckle pattern. The deformed images corresponding to stress values in the range of 50-150 MPa (below yield point) were identified and the average of full-field strain was measured for each image using DIC. The measured strains were coupled with their corresponding stresses that were recorded by tensile stage to calculate the elastic modulus of the material based on the regression method. The accuracy of the results was assessed by comparing the elastic modulus computed by DIC with standard elastic modulus obtained from standard tension test in the same range of stress.

3 RESULTS AND DISSCUSION

The effect of the two pit etching reagents on the microstructure of the cast material is presented in Fig. 3. The use of reagent B for pattern making had two distinct disadvantages: sever oxidation of graphite particles due to high amount of hydrogen peroxide content, and too small pit size that could not be used as speckles in the magnifications used in this study (see Fig. 3(b)). The former disadvantage would cause difficulties for distinguishing strains belong to the regions around graphite particles and the later would induce errors in displacement and strain measurement in the DIC. However, these problems were less evident when using reagent A since the amount of hydrogen peroxide was much lower and the pits were larger (Fig. 3(a)). Therefore, it was decided to consider reagent A for generating speckle patterns for the rest of the study.

Table 4 shows the size and distribution of the speckles and the minimum subset size for each pattern group in two magnifications. As it can be inferred, pit etching provided smaller size and denser pattern compare to natural microstructure pattern in un-etched condition. Moreover, increasing the etching temperature increased the density of pits and reduced NND and pits' size. Nevertheless, pit etching at 75 and 100°C showed almost the same results. It can be interpreted that temperatures higher than 75°C had negligible effect on the number

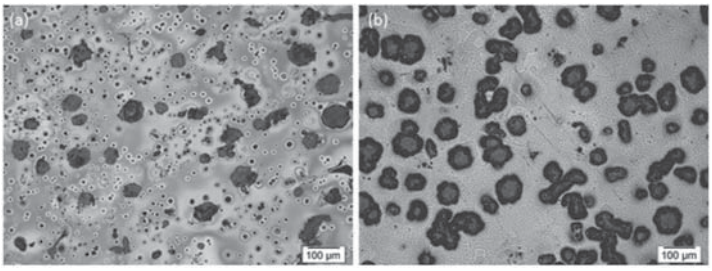

Fig. 3 The microstructure of the cast material pit etched with (a) reagent A, (b) reagent B. Images were taken in 63X magnification.

and size of pits. This can be attributed to the faster evaporation of pit etching reagent on the surface of the material that degraded the efficiency of pitting. The standard deviations (SD) presented for NND and mean radius were calculated based on all the value sobtained from the speckles within a group of speckle pattern and were used for subset size calculation based on the random walk rule. The SD values were used to be in the confidence margin for subset size selection in all similar pit etching procedures. However, in density results SD were considered the deviation of the average density values for every sample within a group of speckle pattern that showed the reliability of the pit etching procedure after each time repeating. Accordingly, the small SD of density values indicated a good reliabilityof pit etching procedure for speckle generating. Figure 4 shows the speckle patterns provided by graphite particles and pit etching at 75°C with the calculated minimum subset sizes.

Table 4 Size and distribution of the speckles and the minimum subset size calculated for each speckle pattern.

	Un-etched	*Pit etched at room temperature*	*Pit etched at 50°C*	*Pit etched at 75°C*	*Pit etched at 100°C*
Mean Radius (µm)	16.5 ± 7.2	3.7 ± 1.7	2.8 ± 1.3	2.7 ± 0.9	2.6 ± 1
Average area(µm²)	1089.4 ± 105	48.4 ± 6.2	31,1 ± 5,1	27.5 ± 3.1	26.4 ± 3.4
Nearest neighbor distance (NND) (µm)	48.3 ± 20.3	22.1 ± 10	11.8 ± 3.9	8.6 ± 2.1	7.9 ± 2.6
Density (number/mm²)	81 ± 7	486 ± 29	2405.1 ± 128	5286.1 ± 362	5444 ± 208
Minimum subset size for 15.8X (pixels)	85 × 85	33 × 33	19 × 19	13 × 13	13 × 13
Minimum subset size for 63X (pixels)	341 × 341	133 × 133	71 × 71	51 × 51	51 × 51

In DIC measurements, speckle patterns play a critical role to ensure a suitable balance between measurement accuracy (bias error) and precision (standard deviation error) [31]. The use of high-contrast small speckles is favorable in order to obtain as many edges aspossible in a small subset sizeand obtain higher spatial resolution together with an accurate gradient measurement during deformation. However, there is a practical limit in size of speckles that the image's speckles should be sampled at least by a 33 pixel array. If the speckle sizes become

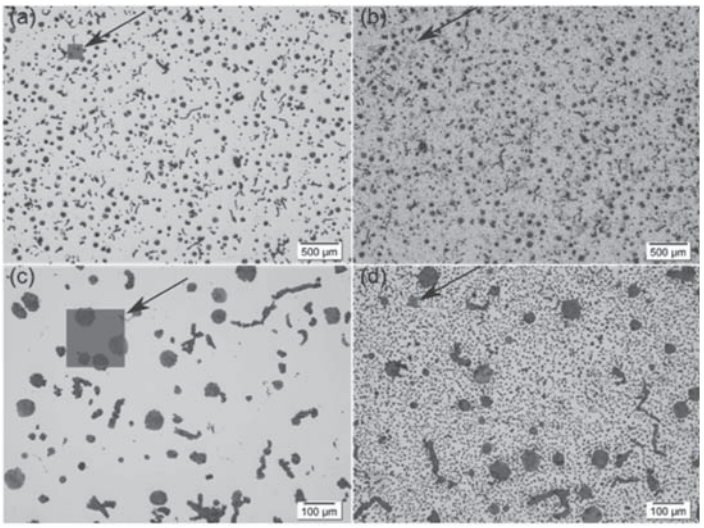

Fig. 4 (a)&(c) Natural microstructural pattern in un-etched condition, (b)&(d) pit etched pattern at 75°C. The top and bottom images correspond to 15.8X and 63X nominal magnifications, respectively. Thesquares that were pointed by the arrowsshow the minimum subset size calculated for each speckle pattern.

smaller than this limit, the camera sensors cannot properly sample the speckles' light signals for image production and eventually the correlation results for these images will severely suffer from aliasing and low contrast bias errors [27, 32]. Here, the area covered with 33 array of pixels for 15.8X and 63X magnifications were 43.16 and 2.62 μm^2, respectively. Comparing with the speckles' average area presented inTable 4, the average area of speckles for all groups in 63X magnification were larger than the limit size indicating that all the speckle sizes were suitable for this magnification. In contrary, for the 15.8X magnification, the average sizes of speckles obtained in high temperature pit etching were smaller than the limit size for this magnification (43.16 μm^2). Thus, speckle patterns produced by high temperature pit etching could not be approved for DIC tests and only natural microstructure pattern and pit etching at room temperature wereused.

Figure 5 shows the displacement and strain spatial resolution and standard deviation that were measuredby using the patterns' minimum subset size. It is clear that the displacement and strain spatial resolution were significantly improved by using pit etching pattern in both magnifications, also by increasing the temperature of pit etching. This was due to the possibility ofthe use of smaller subset sizes in higher temperature pit etching patterns. Displacement spatial resolutions in both magnifications were the same since it was only related to the subset size and the pattern characterization. Strain spatial resolution values were smaller in 63X magnification due to the larger field of view and they had been improved by using smaller subset size (Eq. 3). On the other hand, the standard deviation errors in both displacement and strain were increased by using higher temperature pit etching patterns. This was due to the fact that the standard deviation error increases by decreasing the subset size [25, 26, 30]. The small error bars for standard deviation errors demonstrated the good reliability of the produced patterns in DIC measurements.

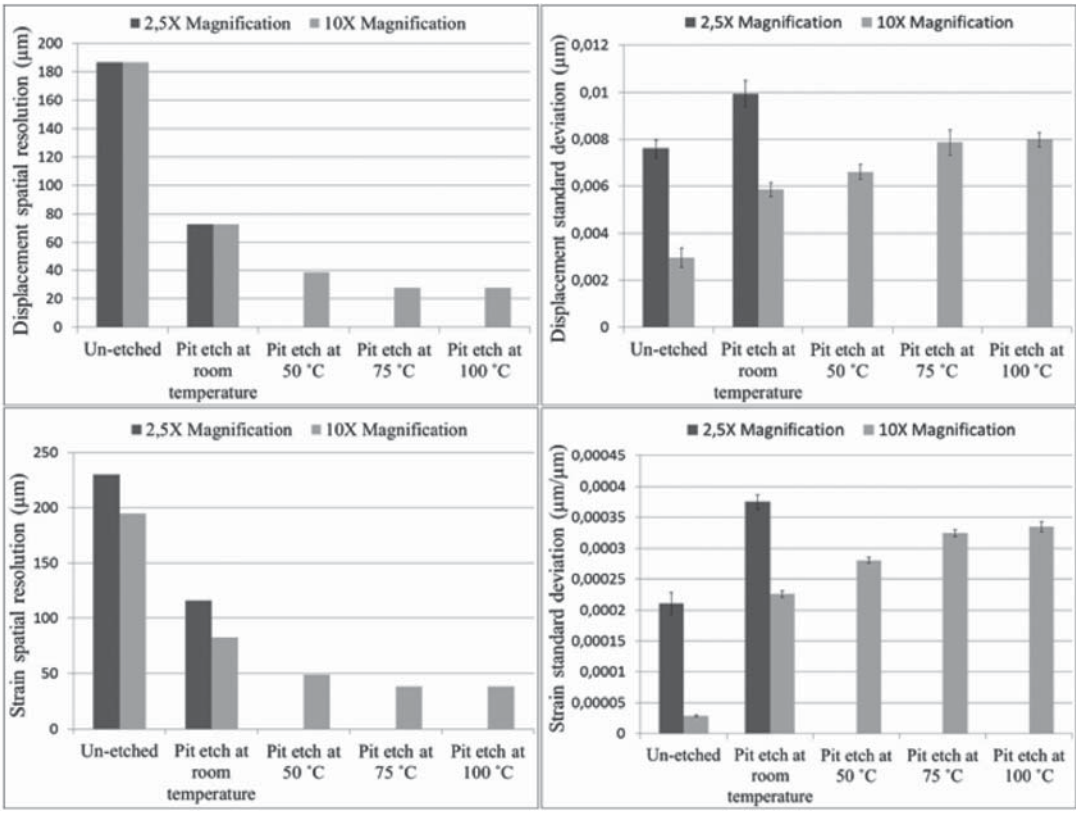

Fig. 5 Strain and displacement spatial resolution and standard deviation that were obtained by patterns' minimum subset size.

In addition, it can be inferred that the selection of a subset size was crucial for the optimum performance of the DIC. Subset sizes smaller than the calculated minimum subset size would increase the errors since subsets were not large enough to contain three speckles in the whole field of view. On the other hand, larger subset sizes would mask the underneath deformation and degrade the accuracy of local heterogenous deformation. However, they could be used in the case of homogenous deformation in trade of sacrificing spatial resolution [33].

For the strain results presented in Fig. 5, the VSG (Eq. 4) was selected to deliver a reasonable small spatial resolution around graphite particles with an acceptable standard deviation. Like subsets, selecting a larger VSG, results in lower gradient detection and smaller standard deviation. This is because in alarger VSG a larger area of displacement data points is considered for strain measurements (more smoothing). Accordingly, in the case of homogeneous deformation a large VSG is preferred to decrease the errors emerged from the displacement field, while for heterogenous deformations a small VSG is more likely to recover more localized data in trade of the more error involvement. Step size can also affect the accuracy and precision of DIC since it prescribes the data density of the displacement field. For a fixed VSG, smaller step size means higher displacement data density for strain calculation which results in a better recovery of real strain field of the area. However, more errors of the displacement data will involve in

smaller step sizes [26, 30]. Accordingly, a larger VSG (higher smoothing) than the one used in the self-correlation test was used in DIC analysis of images acquired from in-situ tensile tests to reduce errors induced from homogeneous elastic deformation. Therefore, the step size and strain window were selected as 5 and 1515 pixels (VSG = 7171 pixels), respectively. However, for images with natural microstructural pattern taken in 63X magnification, step size was defined as 50 pixels due to the necessity of using a large subset size.

In this study, the pattern with the lowest strain spatial resolution was favorable to enable localized strain measurements around and in between graphite particles. In 15.8X magnification, speckle pattern relating to the room temperature pit etching showed the best results in case of speckles size, spatial resolution and standard deviation so that it was decided to be used for in-situ tensile testing. In 63X magnification, the best spatial resolution was achieved by pit etching at 75 and 100°C. Consequently, in-situ tensile testing was performed on samples containing natural microstructure and pit etching in room temperature patterns for 15.8X magnification and natural microstructural and pit etching at 75°C patterns for 63X magnification to assess the accuracy of the minimum subset size for calculating the elastic modulus.

As can be seen in Fig. 6, the elastic modulus values obtained from DIC werein agree with standard testresults with a good approximation. This was attributed to the correct selection of subset size. In addition, it validated the measured localized strain values. Although the same results were obtained for elastic modulus for all the patterns, pit etching pattern enabled much better spatial resolution and can be used for determination of heterogeneous strain fields in regions around graphite particles. This gradient detection was not possible by using natural microstructural pattern. Correspondingly, Fig. 7 represents an example of DIC results obtained in 63X magnification for two in-situ tensile test samples with natural microstructural and pit etching pattern. The improvement in spatial resolution by using smaller subset size can be easily perceived by comparing the strain results. The use of pits as speckle pattern caused better spatial resolution and local gradient detection by creating the possibility of using smaller subset size.

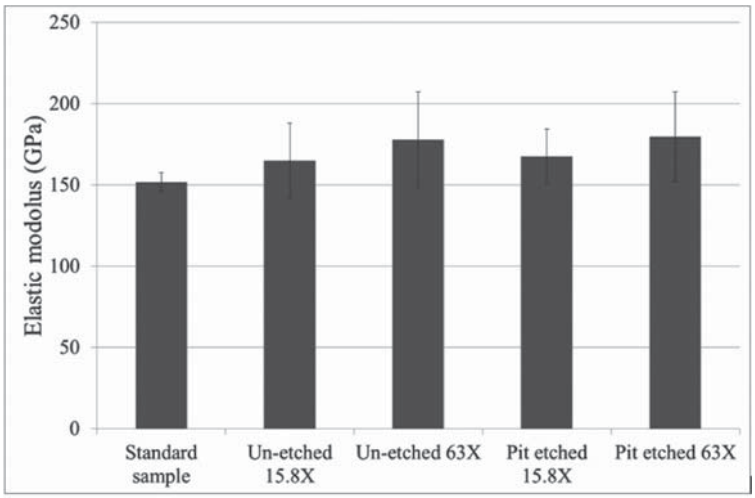

Fig. 6 Comparison between elastic modulus results obtained from DIC analysis and standard tensile test.

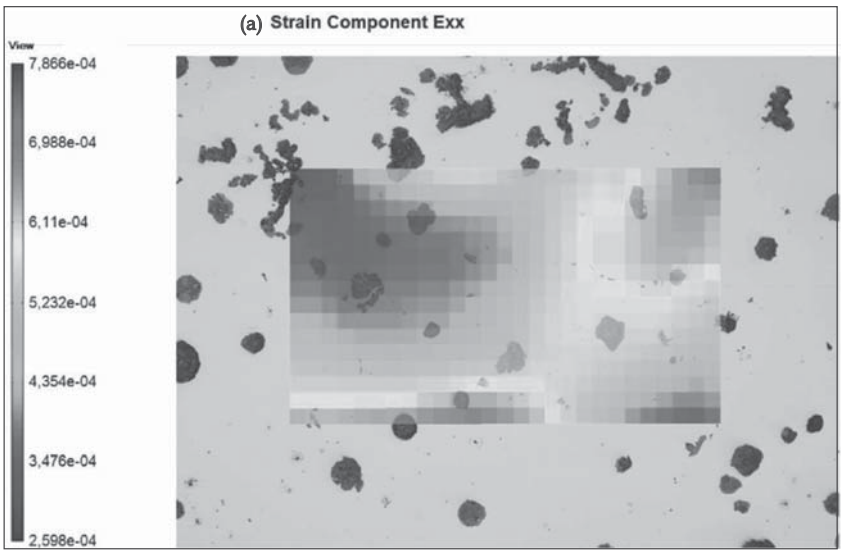

(a)

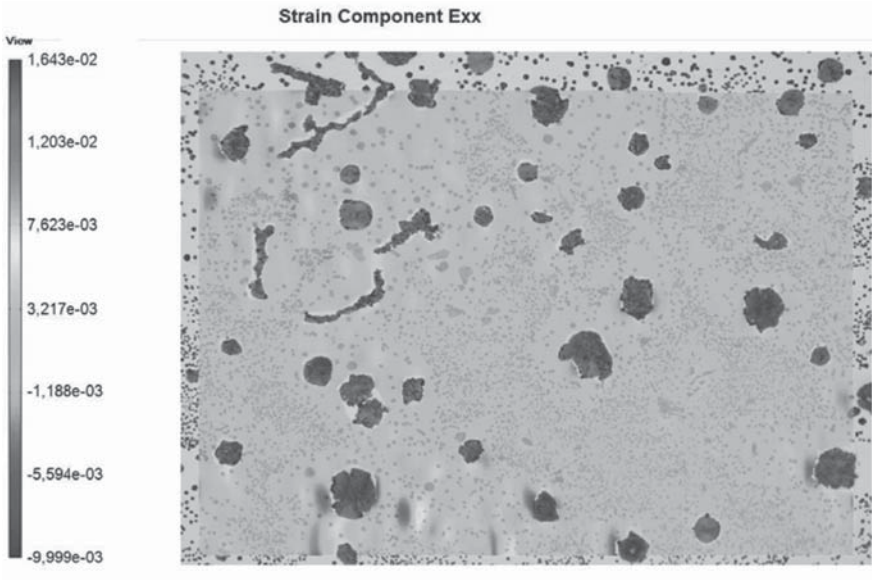

(b)

Fig. 7 Example of DIC strain results for images that were captured in stress values close to 150 MPa with 63X nominal magnification using: (a) natural microstructural pattern, (b) pit etching at 75°C. Scale bars show the strain values.

In contrary, the necessity of using large subsets for natural microstructural pattern (Fig. 7(a)) haddegraded the gradient detection and disabled the detection of strain for a large area near the borders of the image.

In addition to providing higher spatial resolution, the pit etching procedure for speckle generating can be considered a cheap and fast pattern making method without requiring expensive equipment. Furthermore, there would be no debonding between the speckles and surface of the material and the applied pattern does not mask the underlying microstructural features. The pattern can be applied on delicate samples with different geometries since the samples only need to be heated and immersed in the etching reagent. However, the etching reagent contains H_2O_2 and HCl which are hazardous and strongly demands special precautions before usage.

4 CONCLUSIONS

A pit etching procedure was successfully developed and applied to generate speckle patterns suitable for DIC to measure the localized strain values in microstructure of ferritic cast iron. Two pit etching reagents (A and B in Table 2) wereexamined. It was observed that the high amount of hydrogen peroxide in reagent B caused severe corrosion of graphite particles and destruction of the microstructure. Therefore, the regent A was selected for pattern production. The pit etching procedure was performed in different temperatures and the produced patterns were compared with natural microstructural pattern. Microscopic images revealed that the pit etching procedure generated a reliable micro-sized, high contrast, dense and randomly scattered speckles on the surface of the cast material. The minimum subset size for DIC measurements was determined systematically based on the size and distribution of the speckle patterns. The DIC results showed that using the patterns produced by pit etching significantly increased the displacement and strain spatial resolution compared to the use of natural microstructural pattern.

A good fit was found between the elastic modulus measured by the standard tensile test and with the aid of DIC for both natural microstructural pattern and pit etched patterns. This confirmed the accuracy of the calculated minimum subset size andthe local strain measured by DIC. The DIC deformation measurements showed that unlike the natural microstructural pattern the pit patterns enabled the measurement of the strain gradients around the graphite particles, which are known as critical regions for crack initiation. The computed deformation using this pattern making procedure can be used for validation of models.

RFERENCES

1. Sutton, M., et al., *Application of an optimized digital correlation method to planar deformation analysis.* Image and vision computing, 1986. 4(3): pp. 143-150.
2. Sun, Z., J.S. Lyons, and S.R. McNeill, *Measuring microscopic deformations with digital image correlation.* Optics and Lasers in Engineering, 1997. 27(4): pp. 409-428.
3. Sutton, M., et al., *Determination of displacements using an improved digital correlation method.* Image and vision computing, 1983. 1(3): pp. 133-139.
4. Bruck, H., et al., *Digital image correlation using Newton-Raphson method of partial differential correction.* Experimental Mechanics, 1989. 29(3): pp. 261-267.

5. Scrivens, W., et al., *Development of patterns for digital image correlation measurements at reduced length scales.* Experimental Mechanics, 2007. 47(1): pp. 63-77.
6. Ghassemali, E., et al., *Experimental and Simulation of Friction Effects in an Open-Die Microforging/Extrusion Process.* Journal of Micro and Nano-Manufacturing, 2014. 2(1): pp. 011005.
7. Kammers, A. and S. Daly, *Small-scale patterning methods for digital image correlation under scanning electron microscopy.* Measurement science and technology, 2011. 22(12): pp. 125501.
8. Berfield, T., et al., *Micro-and nanoscale deformation measurement of surface and internal planes via digital image correlation.* Experimental Mechanics, 2007. 47(1): pp. 51-62.
9. Nicoletto, G., et al., *Application of high magnification digital image correlation technique to micromechanical strain analysis.* Strain, 2011. 47(s1): pp. e66-e73.
10. Pulos, G., *Use of digital image correlation to determine the mechanical behavior of materials.* Materials Characterization, 2008. 59(11): pp. 1572-1579.
11. El Bartali, A., V. Aubin, and S. Degallaix, *Fatigue damage analysis in a duplex stainless steel by digital image correlation technique.* Fatigue & Fracture of Engineering Materials & Structures, 2008. 31(2): pp. 137-151.
12. Sjögren, T., P.E. Persson, and P. Vomacka, *Analysing the deformation behaviour of compacted graphite cast irons using digital image correlation techniques.* Key Engineering Materials, 2011. 457: pp. 470-475.
13. Reu, P.L. and T.J. Miller, *Experimental validation of equations for 2D DIC uncertainty quantification*, in *Application of Imaging Techniques to Mechanics of Materials and Structures, Volume 4*2013, Springer. pp. 299-305.
14. Pan, B., et al., *Two-dimensional digital image correlation for in-plane displacement and strain measurement: a review.* Measurement science and technology, 2009. 20(6): pp. 062001.
15. Di Cocco, V., F. Iacoviello, and M. Cavallini, *Damaging micromechanisms characterization of a ferritic ductile cast iron.* Engineering Fracture Mechanics, 2010. 77(11): pp. 2016-2023.
16. Baudin, T., et al., *Microtexture determination in Fe-Si alloy sheets by etch pitting. Comparison with the electron back-scattering pattern technique.* Journal of applied crystallography, 1994. 27(6): pp. 924-933.
17. Fortunati, S., G.C. Abbruzzese, and P.E. Di Nunzio. *An etch-pitting technique for statistical analysis of grain size distributions as a function of orientation in Fe-Si alloys*. in *Materials Science Forum*. 1992. Trans Tech Publ.
18. Labrecque, C. and M. Gagné, *Review ductile iron: fifty years of continuous development.* Canadian Metallurgical Quarterly, 1998. 37(5): pp. 343-378.
19. *ASTM Standard E2567-13a, 2013,"Standard Test Method for Determining Nodularity And Nodule Count In Ductile Iron"*, in *ASTM Internationals, West Conshohocken, PA, 2013, DOI:10.1520/E2567–13A, www.astm.org.*
20. Davis, J.R., *Tensile testing*2004: ASM international.

21. *ASTM Standard E8/E8M, 2013,"Standard Test Methods for Tension Testing of Metallic Materials"*, in *ASTM Internationals, West Conshohocken, PA, 2013, DOI:10.1520/ E0008_E0008M-13A, www.astm.org.*
22. Tanaka, T. and M. Kosugi, *Crystallographic study of the fatigue crack nucleation mechanism in pure iron.* Basic Questions in Fatigue., 1984. 1: pp. 98-119.
23. Beguinot, J. and P. Lesbats, *A new reagent for etch pits in silicon steel.* Metallography, 1977. 10(1): pp. 115-119.
24. Lava, P., et al., *Assessment of measuring errors in DIC using deformation fields generated by plastic FEA.* Optics and Lasers in Engineering, 2009. 47(7): pp. 747-753.
25. Pan, B., et al., *Study on subset size selection in digital image correlation for speckle patterns.* Optics express, 2008. 16(10): pp. 7037-7048.
26. Wang, Y., et al., *Investigation of the uncertainty of DIC under heterogeneous strain states with numerical tests.* Strain, 2012. 48(6): pp. 453-462.
27. Sutton, M.A., J.J. Orteu, and H. Schreier, *Image correlation for shape, motion and deformation measurements: Basic Concepts, Theory and Applications*2009: Springer.
28. Spitzer, F. and A. Mathematician, *Principles of random walk*1964: Springer.
29. Wang, Z., et al., *Statistical analysis of the effect of intensity pattern noise on the displacement measurement precision of digital image correlation using self-correlated images.* Experimental Mechanics, 2007. 47(5): pp. 701-707.
30. Lava, P., S. Cooreman, and D. Debruyne, *Study of systematic errors in strain fields obtained via DIC using heterogeneous deformation generated by plastic FEA.* Optics and Lasers in Engineering, 2010. 48(4): pp. 457-468.
31. Pan, B., Z. Lu, and H. Xie, *Mean intensity gradient: an effective global parameter for quality assessment of the speckle patterns used in digital image correlation.* Optics and Lasers in Engineering, 2010. 48(4): pp. 469-477.
32. Lecompte, D., et al., *Quality assessment of speckle patterns for digital image correlation.* Optics and Lasers in Engineering, 2006. 44(11): pp. 1132-1145.
33. Yaofeng, S. and J.H. Pang, *Study of optimal subset size in digital image correlation of speckle pattern images.* Optics and Lasers in Engineering, 2007. 45(9): pp. 967-974.